

**Dieses Dokument ist eine Zweitveröffentlichung (Postprint) /**

**This is a self-archiving document (accepted version):**

Shunqi Xu, Marcus Richter, Xinliang Feng

**Vinylene-Linked Two-Dimensional Covalent Organic Frameworks:  
Synthesis and Functions**

**Erstveröffentlichung in / First published in:**

*Accounts of Materials Research.* 2021, 2(4), S. 252-265 [Zugriff am: 14.04.2022]. ACS Publications. ISSN 2643-6728.

DOI: <https://doi.org/10.1021/accountsmr.1c00017>

Diese Version ist verfügbar / This version is available on:

<https://nbn-resolving.org/urn:nbn:de:bsz:14-qucosa2-788358>

# Vinylene-Linked Two-Dimensional Covalent Organic Frameworks: Synthesis and Functions

*Shunqi Xu, Marcus Richter, Xinliang Feng \**

Technische Universität Dresden, Center for Advancing Electronics Dresden (cfaed) and Faculty of Chemistry and Food Chemistry, Chair of Molecular Functional Materials, Mommsenstraße 4, 01069 Dresden (Germany).

**KEYWORDS.** Vinylene-linked, Two-dimensional covalent organic frameworks

**Conspectus:** Two-dimensional covalent organic frameworks (2D COFs) with covalently bonded repeat units and crystalline, porous framework backbones have attracted immense attention since the first 2D COFs were reported by Yaghi's group in 2005. The extended single-layered structures of 2D COFs are also generally considered as the 2D polymers. The precise incorporation of molecular building blocks into ordered frameworks enables the synthesis of novel organic materials with designable and predictable properties for specific applications, such as in optoelectronics, energy storage and conversion. In particular, the 2D  $\pi$ -conjugated COFs (2D-c-COFs) represent a unique class of 2D conjugated polymers that have 2D molecular-periodic structures with extended in-plane  $\pi$ -conjugations. In the 2D-c-COFs, the conjugated skeletons and  $\pi$ - $\pi$  stacking interactions can provide the pathways for electron transport, while the porous channel can enable loading active sites for catalysis and sensing. Thus far, the synthesis of 2D-c-COFs has

been mostly limited to the Schiff-base chemistry based on the condensation reaction between amine and aldehyde/ketone monomers, because the construction of 2D COFs as thermodynamically controlled products generally requires a highly reversible reaction for error-correction processes. However, the high reversibility of imine linkages would conversely endow moderate  $\pi$ -electron delocalization due to the polarized carbon-nitrogen bonds and poor stability against strong acids/bases.

To achieve robust and highly conjugated 2D-c-COFs, a series of synthetic strategies have been developed, including one-step reversible reaction with bond form-broken-reform function, quasi-reversible reaction combining reversible and irreversible processes, and post-modifications converting labile bonds to a robust linkage. Among all the reported 2D-c-COFs, vinylene-linked (also  $sp^2$ -carbon-linked) 2D covalent organic frameworks (V-2D-COFs) with high in-plane  $\pi$ -conjugation have attracted increasing interest after we reported the first V-2D-COFs via a Knoevenagel polycondensation in 2016. Although C=C bonds have low reversibility making the synthesis of V-2D-COFs quite challenging, there have been around 40 V-2D-COFs reported over the past five years, which demonstrated the merits of V-2D-COFs combining with unique optoelectronic, redox, and magnetic properties.

In this Account, we will summarize the development of V-2D-COFs, covering the important aspects of synthetic methods, design strategies, unique physical properties and functions. First, the solvothermal synthesis of V-2D-COFs using different reaction methodologies and design principles will be presented, including Knoevenagel polycondensation, other aldol-type polycondensations, and Horner-Wadsworth-Emmons (HWE) polycondensation. Second, we will discuss the optoelectronic and magnetic properties of V-2D-COFs. Finally, the promising

applications of V-2D-COF in the fields of sensing, photocatalysis, energy storage and conversion will be demonstrated, which benefit from their robust vinylene-linked skeleton, full in-plane  $\pi$ -conjugation, and tailorable structures. We anticipate that this Account will provide an intensive understanding of the synthesis of V-2D-COFs and inspire the further development of this emerging class of conjugated organic crystalline materials with unique physicochemical properties and applications across different areas.

## 1. Introduction

Two-dimensional  $\pi$ -conjugated covalent organic frameworks (2D-c-COFs), which can be generally classified as a unique type of 2D conjugated polymers, are characterized by layer-stacked periodic frameworks with remarkable in-plane  $\pi$ -conjugations.<sup>1-3</sup> In 2011, the first successful solution-synthesis of 2D-c-COF was achieved via Schiff-base condensation between tetra(p-amino-phenyl)porphyrin (TAPP) and terephthalaldehyde.<sup>4</sup> Later, Schiff-base chemistry<sup>5</sup> was adapted for the synthesis of 2D-c-COFs containing hydrazone<sup>6</sup> or azine.<sup>7,8</sup> However, imine-linked 2D-c-COFs generally undergo hydrolysis under strong acidic/basic conditions.<sup>9,10</sup> Moreover, the highly polarized carbon-nitrogen bond in the abovementioned linkages cannot promote efficient  $\pi$ -electron delocalization through the 2D conjugated skeleton, which results in moderate optoelectronic properties.<sup>11-13</sup> As a result, the implementation of 2D-c-COFs in optoelectronic applications remains limited. Therefore, it is highly desirable to develop a new class of 2D-c-COFs with extensive 2D  $\pi$ -conjugation that can truly bridge the world of 2D conjugated polymers with both exceptional electronic and optoelectronic properties.

Among the efforts to achieve robust and highly conjugated 2D-c-COFs, vinylene-linked 2D COFs (named V-2D-COFs) have attracted rapidly growing interest since the first example was prepared via Knoevenagel polycondensation in 2016 by us and shortly afterward by Jiang.<sup>14,15</sup> The excellent  $sp^2$ -carbon-linked  $\pi$ -conjugation along the 2D skeleton makes V-2D-COFs promising semiconductors for a number of applications, such as in sensing,<sup>16,17</sup> energy conversion,<sup>12,18</sup> and energy storage<sup>9</sup>. Nevertheless, the synthesis of highly crystalline V-2D-COFs remains challenging, since the formation of vinylene linkages is principally irreversible,<sup>14</sup> in contrast to the well-explored imine chemistry with high reversibility.<sup>2,19</sup> In addition to Knoevenagel polycondensation, other aldol-type polymerizations between aromatic aldehydes and electron-deficient mesitylene derivatives have recently been utilized to synthesize unsubstituted V-2D-COFs.<sup>20–22</sup> In 2020, our group reported the Horner-Wadsworth-Emmons (HWE) polymerization to achieve unsubstituted V-2D-COFs using aromatic aldehyde and phosphonate monomers.<sup>23</sup>

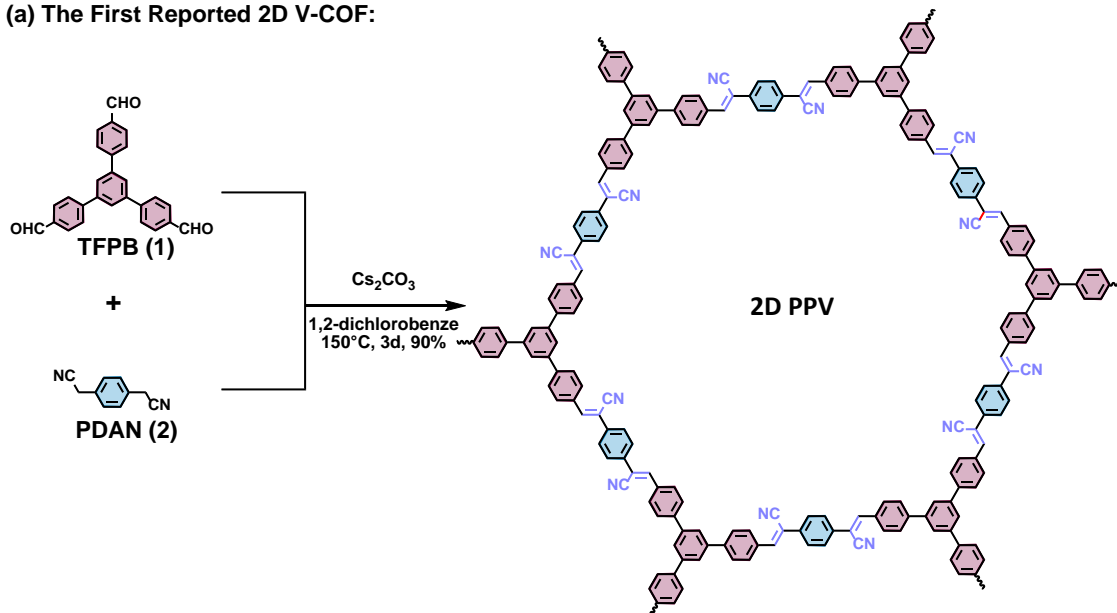
In this Account, we summarize the recent achievements related to V-2D-COFs in terms of synthetic methods and design strategies, unique physical properties and functions. In the first section, we will present the solvothermal syntheses of V-2D-COFs, including Knoevenagel, other aldol-type and HWE polycondensations. Subsequently, we will discuss the unique (opto)electronic and magnetic properties of V-2D-COFs as well as their inherent functional applications in photocatalysis and energy storage. Finally, we will provide an outlook about the challenges and future development of V-2D-COFs concerning the reaction methods, structural designs and new potential applications.

## 2. Chemical Methods

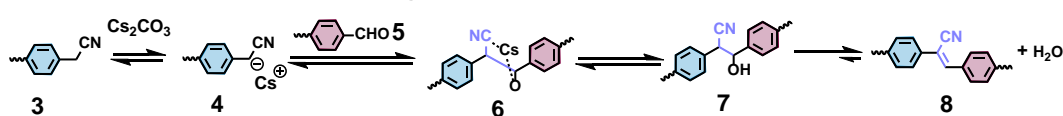
### 2.1. Knoevenagel Polycondensation

In 2016, the first cyano-substituted V-2D-COF (Figure 1a) was synthesized via  $\text{Cs}_2\text{CO}_3$ -catalyzed Knoevenagel condensation between  $\text{C}_3$ -symmetrical 1,3,5-tris(4-formylphenyl)benzene (TFPB, 1) and  $\text{C}_2$ -symmetrical *p*-phenylenediacetonitrile (PDAN, 2).<sup>14</sup> Importantly, the resultant V-2D-COF was recognized as a 2D poly(phenylenevinylene) (2D PPV) derivative with part of the cross-conjugation due to the TFPB motif. The formation of cyano-vinylene linkages was identified by solid-state  $^{13}\text{C}$ -NMR and infrared (IR) spectroscopy. Powder X-ray diffraction (PXRD) analysis of 2D PPV with a synchrotron radiation source indicated an ordered structure on the basis of the assignment of the first three diffractions to the (110), (020) and (220) reflections. To gain a deeper understanding on this 2D polymerization method, different bases, including  $\text{Na}_2\text{CO}_3$ ,  $\text{NaOH}$ ,  $\text{K}_2\text{CO}_3$  or  $\text{CsF}$ , were further screened for the Knoevenagel reaction.<sup>24</sup> Interestingly, only  $\text{Cs}_2\text{CO}_3$ -catalyzed conditions could generate the model compound in a high yield of 84%. Further density functional theory (DFT) calculations examined the energy profile for the mechanism of a model reaction between 2-phenylacetonitrile (3) and benzaldehyde (5) (Figure 1b), which suggests that the  $\text{Cs}^+$  ion can stabilize the carbanion intermediate (6) by forming a five-membered transition state by bridging with oxygen and nitrogen, endowing quasi-reversible C-C bond formation in the first step. In the last five years, several aromatic aldehyde monomers and acetonitrile with different geometries have been successfully implemented in the synthesis of cyano-substituted V-2D-COFs, such as  $\text{C}_3$ -symmetrical 2,3,8,9,14,15-hexa(4-formylphenyl)diquinoxalino[2,3-a:2',3'-c]phenazine (HATN-6CHO, 10),<sup>9</sup>  $\text{C}_4$ -symmetrical tetrakis(4-benzaldehyde)porphyrin (*p*-Por-CHO, 12),<sup>25</sup> and  $\text{C}_3$ -symmetrical 2,4,6-tris(4-formylphenyl)-1,3,5-triazine (TFPT, 13),<sup>26</sup> as well as  $\text{C}_2$ -symmetrical 2,2'-bipyridine-based 5,5-bis(cyanomethyl)-2,2'-bipyridine (BCBP, 16),<sup>27</sup> and 2,2'-([2,2'-bithiophene]-5,5'-diyl)diacetonitrile (ThDAN, 17)<sup>12</sup> (Figure 1c and 1d).

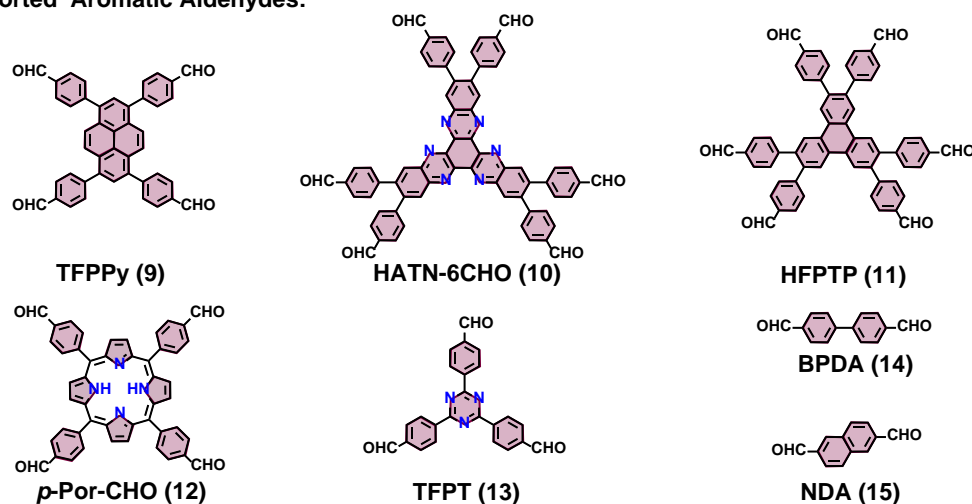
**(a) The First Reported 2D V-COF:**



**(b) Proposed Mechanism for Knoevenagel Condensation:**



**(c) Reported Aromatic Aldehydes:**



**(d) Reported Aromatic Methylene Nitrile:**

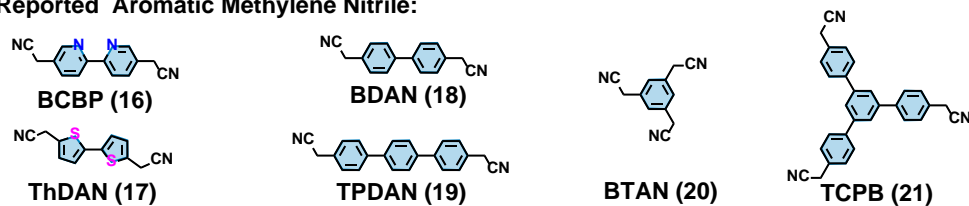


**Figure 1.** (a) Synthesis of the first cyano-substituted V-2D-COF (2D PPV) via Knoevenagel condensation between TFPB (1) and PDAN (2). (b) Proposed mechanism of Knoevenagel condensation between aryl methylene nitrile (3) and aryl aldehyde (5) to cyano-substituted trans-vinylenes (8) with  $\text{Cs}_2\text{CO}_3$  as the base. (c) Reported aromatic aldehyde functionality for the synthesis of cyano-substituted V-2D-COFs. (d) Reported aromatic methylene nitrile for the synthesis of cyano-substituted 2D V-COFs.

Based on the abovementioned examples, Knoevenagel polycondensation is a versatile reaction method for the synthesis of V-2D-COF due to the availability of various functional monomers. However, a comprehensive screening of the reaction conditions is required for the synthesized V-2D-COFs due to the poor reversibility of the reaction. An interesting pathway to promote the formation of crystalline CN-substituted V-2D-COFs is topology-templated Knoevenagel polymerization.<sup>10</sup> In this strategy, the corresponding imine-linked 2D COFs were used as templates to facilitate and confine the growth of the cyano-substituted V-2D-COF onto the x-y plane. Afterwards, crystalline cyano-substituted V-2D-COF was obtained after hydrolyzing the imine-based template. It should be noted that only the use of the template-assisted approach allowed the synthesis of crystalline  $\text{sp}^2\text{c-COF-5}$  (Figure 2), while the direct polymerization approach without using template generated only the corresponding amorphous polymers.

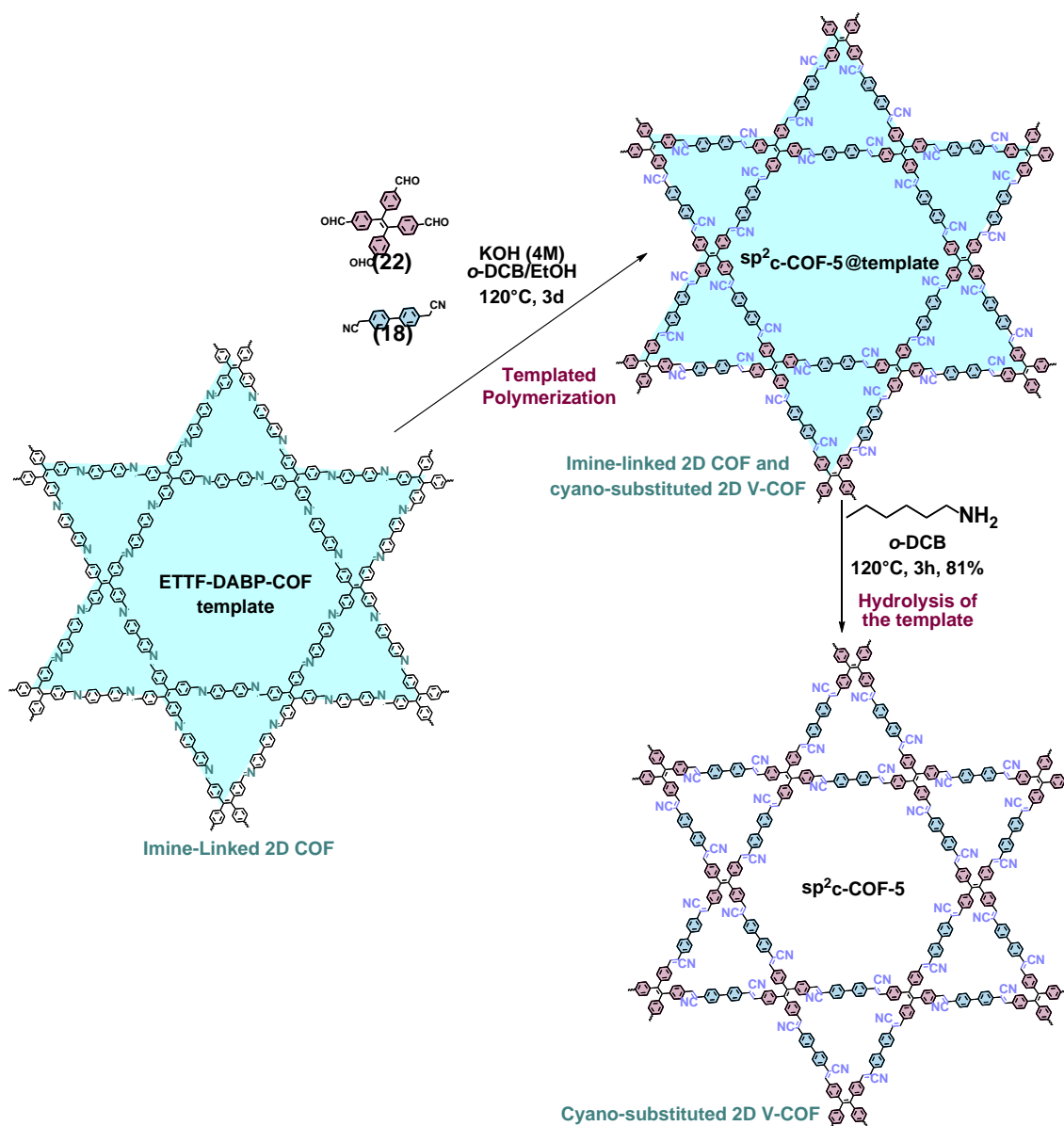


**Figure 2.** Topology-templated synthesis of a kagome V-2D-COF ( $\text{sp}^2\text{c-COF-5}$ ) using an imine-linked 2D COF as a template.

## 2.2 Other Aldol-Type Polycondensations

In contrast to the synthesis of cyano-substituted V-2D-COFs using Knoevenagel 2D polycondensation, other aldol-type polycondensation reactions enable the synthesis of

unsubstituted V-2D-COFs. The first synthesis of an unsubstituted V-2D-COF, namely, COF-701, was achieved by Brønsted acid-catalyzed condensation between 2,4,6-trimethyl-1,3,5-triazine (TMT, 23) and 4,4'-biphenyldicarbaldehyde (BPDA, 14, Figure 3a).<sup>20</sup> A model reaction between TMT (23) and benzaldehyde (4) was first conducted under CF<sub>3</sub>SO<sub>3</sub>H-catalyzed conditions, affording the isolated target compound 2,4,6-tri((E)-styryl)-1,3,5-s-triazine (TST, 26) in 63% yield. The crystallinity of COF-701 was demonstrated by wide-angle X-ray scattering with a staggered (AB) stacking mode. Furthermore, N<sub>2</sub> sorption measurements exhibited a high Brunauer-Emmett-Teller (BET) surface area of 1366 m<sup>2</sup> g<sup>-1</sup> and a pore size distribution of 1.14 nm.

Recently, a one-pot strategy for synthesizing unsubstituted V-2D-COFs from a commercial solvent acetonitrile, combining a cyclotrimerization and an aldol-type condensation, was demonstrated. (Figure 3a).<sup>28</sup> A time-dependent <sup>1</sup>H-NMR study indicated that the protonated TMT (23) was formed under the trifluoromethanesulfonic acid (TfOH) catalyzed trimerization of acetonitrile, with the yield of ~20 % after 1 h. Furthermore, in the presence of benzaldehyde, the isolated yield of the model compound TST was up to 80%. To avoid the possible TfOH catalyzed unwanted radical reaction pathways, a comprehensive screening of solvents was performed, which revealed that the polymerization in a mixture of methanol and acetonitrile at 120 °C could generate highly crystalline COF-701. This multistep sequential reaction provided a new strategy for the preparation of COF materials. However, it should be noted that such method required a more careful control on the reaction conditions for the formation of highly crystalline V-2D-COFs.

Moreover, aldol-type condensations under basic conditions using different bases, such as piperidine, NaOH and dimethylamine, were also developed for the synthesis of crystalline unsubstituted V-2D-COFs.<sup>29–32</sup> By employing the TMT monomer (23) and different aldehydes,

including TFPB (1), BPDA (14), and 1,4-phthalaldehyde (PDA, 28), the structural diversities of V-2D-COFs could be extended. The proposed mechanism comprises three steps (Figure 3b): First, TMT (23) is deprotonated to form a reactive carbanion species due to the electron-withdrawing nature of the nitrogen atoms in the triazine unit (24, Figure 3b). In the second step, the nucleophilic intermediate (24) attacks the aldehyde group of the monomer (4), which leads to the formation of a new C-C bond (25). Subsequent elimination generates water and unsubstituted vinylene linkages (26). Such aldol-type condensations are not limited to TMT (23) (Figure 3c); other electron-deficient mesitylene-type monomers, such as 5-dicyano-2,4,6-trimethylpyridine (DCTMP, 29)<sup>21,29</sup> and trimethyltriazine (TMTA, 30),<sup>22</sup> have also been successfully used for the construction of unsubstituted V-2D-COFs.

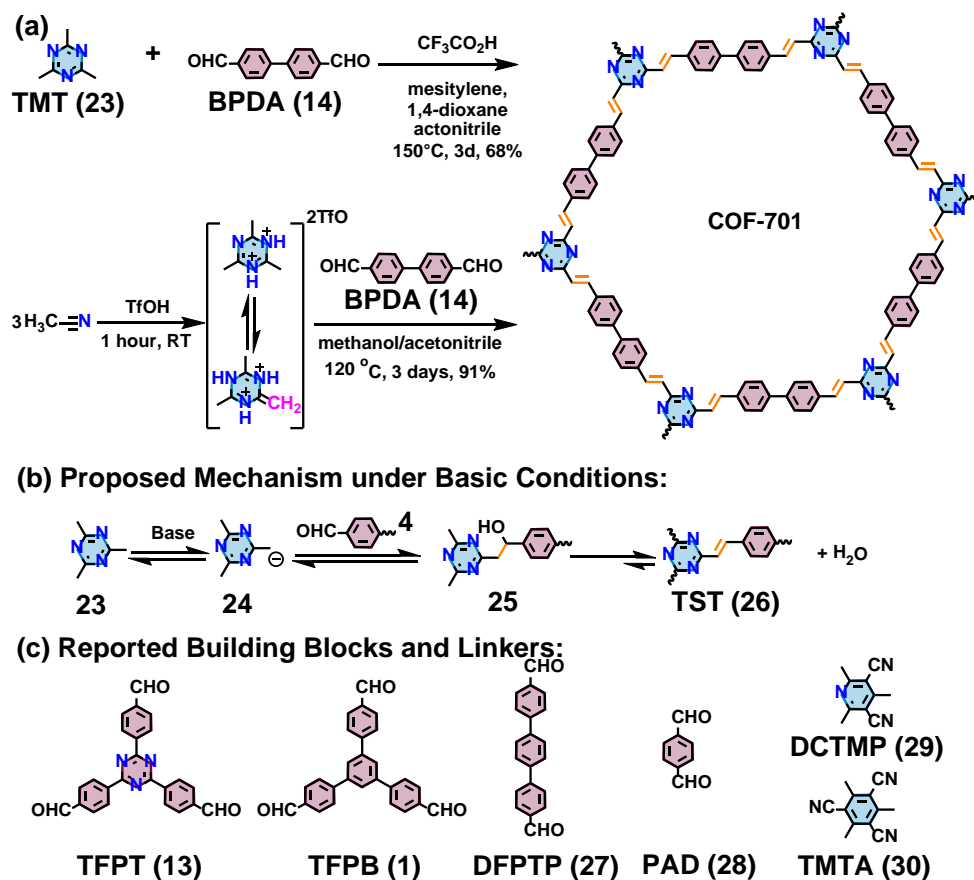


**Figure 3.** (a) Synthesis of unsubstituted V-2D-COF (COF-701) by acid-catalyzed aldol-type condensations between TMT (23) and BPDA (14), and a multistep sequential reaction combining cyclotrimerization and Aldol condensation in one pot. (b) Proposed mechanism of the reaction with TMT (23). (c) Reported electron-deficient mesitylene derivatives and monomers with aldehyde functionality for the synthesis of V-2D-COFs via aldol-type condensation.

### 2.3. Horner–Wadsworth–Emmons (HWE) Polymerization

Another notable reaction methodology for the synthesis of unsubstituted V-2D-COFs is the Horner-Wadsworth-Emmons (HWE) reaction, which was recently demonstrated by our group.<sup>23</sup> In contrast to aldol-type 2D polycondensations, HWE 2D polymerization between aromatic phosphonate and aldehyde is a more robust way to synthesize unsubstituted V-2D-COFs with

different topologies. The model compound 4,4'-di((E)-styryl)-1,1'-biphenyl (33) and the linear polymer poly(phenylenevinylene) (34) were first synthesized under  $\text{Cs}_2\text{CO}_3$ -catalyzed conditions with yields of ~80% and 79%, respectively (Figure 4a and b). The mechanism of the HWE reaction is proposed to involve three steps and a stabilized six-membered cyclic transition state with  $\text{Cs}^+$  (37), which includes an exclusive trans-vinylene bond (39) after the elimination step. Moreover, DFT simulations suggest that C-C single bond formation is reversible (from 35 and 4 to 38), which is crucial for the formation of crystalline V-2D-COFs. V-2D-COFs, namely, 2D poly(phenylenequinoxalinevinylene) 2D-PPQV-1 and 2D-PPQV-2, were obtained via a  $\text{Cs}_2\text{CO}_3$ -catalyzed HWE reaction between HATN-6CHO (10) and 1,4-bis(diethylphosphonomethyl)benzene (BEPB, 40) or 4,4'-bis(diethylphosphonomethyl)biphenyl (BEPP, 41). The PXRD and BET measurements of 2D-PPQV-1 and 2D-PPQV-2 revealed a crystalline 2D framework with a dual-pore structure.

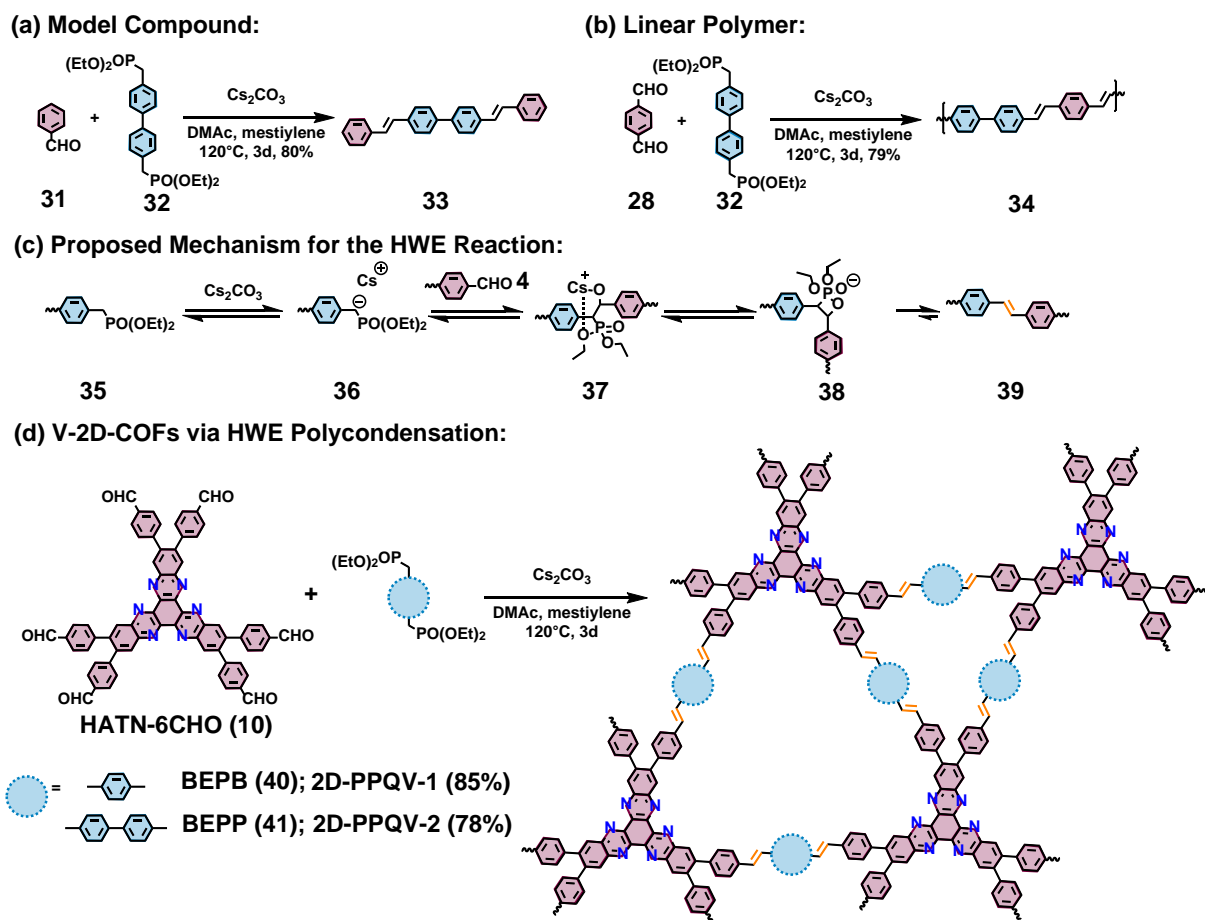


**Figure 4.** (a) Synthesis of the model compound 4,4'-di((E)-styryl)-1,1'-biphenyl (33). (b) Synthesis of a linear polyphenylenevinylene (34). (c) Proposed mechanism of the HWE reaction between aryl phosphonate (35) and aryl aldehyde (4) to form compound 39. (d) Synthesis of 2D-PPQV-1 and 2D PPQV-2 via HWE polymerization.

### 3. Optoelectronic Properties

The high in-plane  $\pi$ -conjugation and access to variable monomers with different topologies enable the exploration of the unique physicochemical properties of V-2D-COFs. For instance, we investigated the optoelectronic properties of 2D-CN-PPV-0, 2D-CN-PPV-1, and 2D-CN-PPV-2 with a hexagonal topology and different pore sizes (Figure 5a).<sup>24</sup> As a result, the UV-vis absorption

spectra of the V-2D-COF dispersions in isopropanol showed absorption maxima at 368, 372, and 384 nm, with corresponding absorption edges of 460, 501, and 488 nm for 2D-CN-PPV-0, 2D-CN-PPV-1, and 2D-CN-PPV-2, respectively (Figure 5b). Consequently, the optical energy gaps of 2D-CN-PPV-1, 2D-CN-PPV-0, and 2D-CN-PPV-2 were estimated to be 2.70, 2.47, and 2.54 eV, respectively. Moreover, the emission maxima of 2D-CN-PPV-1, 2D-CN-PPV-0, and 2D-CN-PPV-2 were observed at 498, 550, and 511 nm, respectively (Figure 5c). These investigations of the structure-property relationship confirmed that the length of the linkers and the corresponding  $\pi$ -conjugation degree strongly influenced the optical energy gaps.

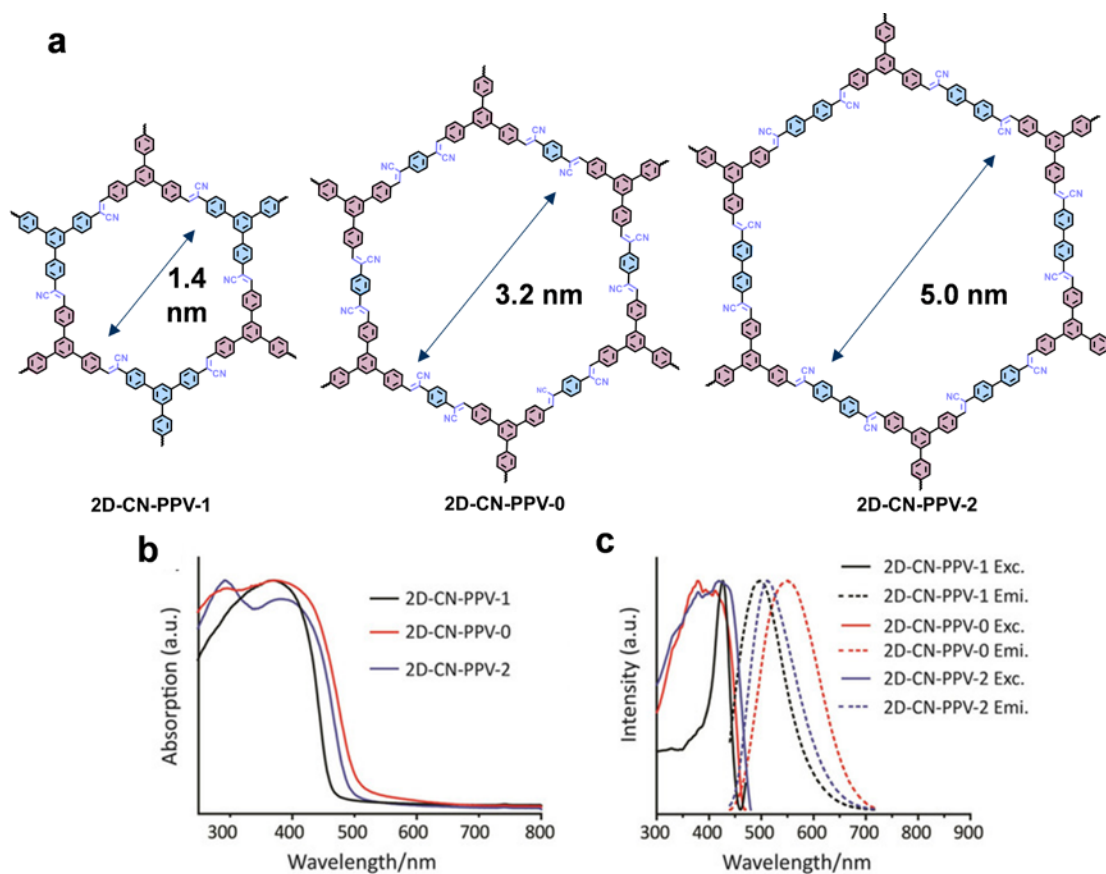


**Figure 5.** (a) Chemical structures of 2D-CN-PPV-0, 2D-CN-PPV-1 and 2D-CN-PPV-2. (b) UV-vis absorption spectra of 2D-CN-PPV-0 (red), 2D-CN-PPV-1 (black) and 2D-CN-PPV-2 (blue) in

isopropanol. (c) Fluorescence spectra of 2D-CN-PPV-0 (red), 2D-CN-PPV-1 (black) and 2D-CN-PPV-2 (blue) in isopropanol. Reproduced with permission from 24. Copyright © 2019 Wiley-VCH Verlag GmbH & Co. KGaA, Weinheim.

To further examine the influence of the vinylene linkages on the optoelectronic properties of V-2D-COFs, HATN-containing cyano-substituted 2D CCP-HATN and unsubstituted 2D-PPQV1 as well as the corresponding imine-linked COF analog (2D C=N HATN) were compared (Figure 6a).<sup>23</sup> The UV-vis absorption spectra exhibited absorption edges at 575, 540, and 598 nm for 2D C=N HATN, 2D CCP-HATN and 2D-PPQV1, respectively (Figure 6b). Thus, the Tauc plots based on the UV-vis absorption spectra revealed optical energy gaps of 2.31, 2.39 and 2.20 eV for 2D C=N HATN, 2D CCP-HATN, and 2D-PPQV-1, respectively. Compared with cyano-substituted 2D CCP-HATN, unsubstituted 2D-PPQV-1 exhibited a lower optical energy gap, which can be attributed to the structural planarity of the vinylene linkages, which can enhance the electron delocalization over the whole  $sp^2$ -carbon-linked backbone. Moreover, the emission spectra indicated significantly different emission behaviors among the above three 2D COFs. As shown in Figure 6c and 6d, the imine-linked 2D C=N HATN displayed negligible fluorescence, while 2D CCP-HATN and 2D-PPQV-1 emitted at 564 and 629 nm, respectively. Compared to that of 2D-PPQV-1, the emission maximum of 2D CCP-HATN was blue shifted, which is caused by the decreased conjugation degree due to the nonplanarity of the cyano-substituted vinylene linkages.

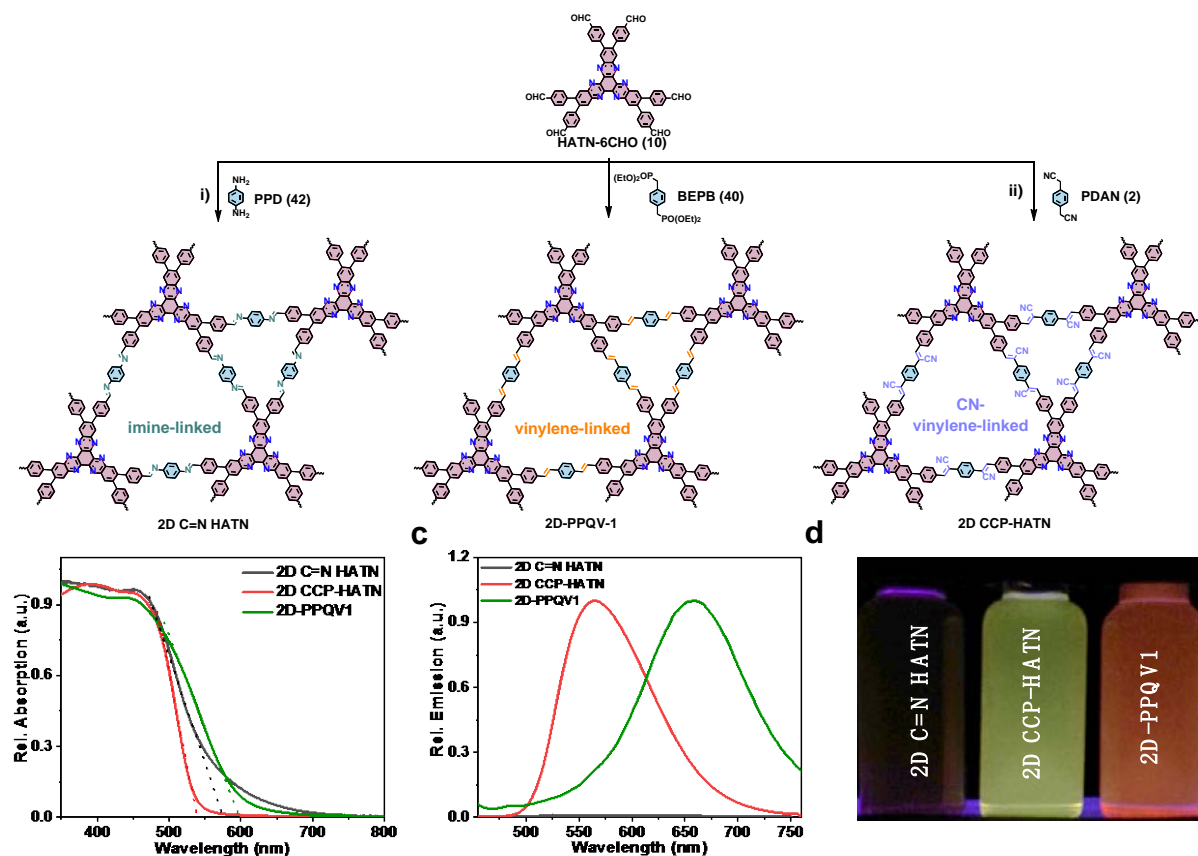


**Figure 6.** (a) Synthetic scheme for 2D C=N HATN, 2D-PPQV-1, and 2D CCP-HATN. Reaction conditions: i) *N,N*-dimethylacetamide (DMAc)/mesitylene (Mes)/acetic acid (HOAc, 6.0 M)=5/5/1, 120 °C. ii) Cs<sub>2</sub>CO<sub>3</sub>, DMAc/*ortho*-dichlorobenzene (*o*-DCB)=2/1, solid Cs<sub>2</sub>CO<sub>3</sub>, 120 °C. iii) DMAc/*o*-DCB=1/1, solid Cs<sub>2</sub>CO<sub>3</sub>, 120 °C. (b) UV-vis absorption and (c) fluorescence spectra of 2D C=N HATN (black), 2D CCP-HATN (red), and 2D-PPQV1 (green) dispersions in 2-propanol (0.2 mg/mL). (d) Photographs of 2D-C=N HATN, 2D CCP-HATN, and 2D PPQV1 under 365 nm UV light. Reproduced with permission from 23. Copyright © 2020 Wiley-VCH GmbH

Moreover, the photoluminescence quantum yields (PLQYs) of the V-2D-COFs were investigated by comparison with the corresponding imine-linked 2D-c-COFs.<sup>33</sup> For instance, triphenylene-containing and cyano-substituted V-2D-COFs, namely, 2D CCP-HFPTP-PDAN and 2D CCP-

HFPTP-BDAN, were synthesized under  $\text{Cs}_2\text{CO}_3$ -catalyzed conditions in 85% and 89% yields, respectively (Figure 7a). The obtained 2D CCP-HFPTP-PDAN and 2D CCP-HFPTP-BDAN exhibited high PLQYs of 24.9% and 32.3%, respectively, which are the highest PLQY values reported for 2D-c-COFs.<sup>16,24,34–39</sup> In contrast to the two CN-substituted V-2D-COFs, the imine-linked 2D C=N HFPTP-PPD exhibited negligible fluorescence. The high PLQY values of both V-2D-COFs can be explained by the steric hindrance between cyano groups and hydrogen atoms in adjacent benzene rings and the consequent restricted intramolecular bond rotation of the cyano-substituted vinylene linkage. Furthermore, the synthesized V-2D-COFs demonstrated high photostability under UV irradiation (36 W) for two hours (Figure 7b). The high photostability of CN-substituted V-2D-COFs can be first explained by the rigid vinylene-linked skeleton, which can significantly impede the photodegradation rates.<sup>40</sup> On the other hand, the shortest distance between the vinylene bonds of adjacent layers is approximately 6.2 and 6.0 Å for 2D CCP-HFPTP-PDAN and 2D CCP-HFPTP-BDAN, respectively (Figure 7c), and these values are much larger than the 4.2 Å that required for interlayer [2+2] photocycloaddition between two vinylene bonds.<sup>41</sup>

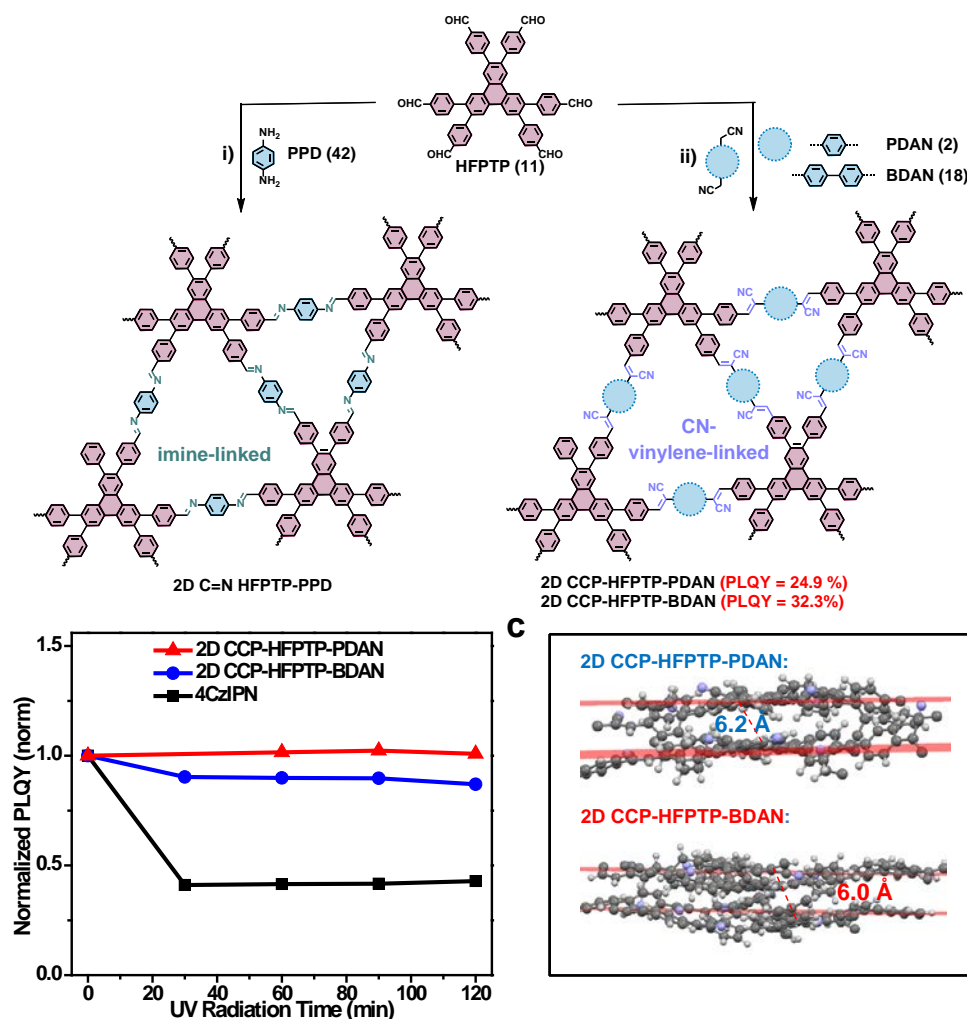


**Figure 7.** (a) Synthetic scheme for 2D CCP-HFFTP-PDAN, 2D CCP-HFFTP-BDAN, and 2D C=N COF-HFFTP-PPD. Reaction conditions: i) DMAc/Mes/HOAc (6.0 M)=5/5/1, 120 °C. ii) and iii) DMAc/*o*-DCB/Cs<sub>2</sub>CO<sub>3</sub> (0.1 M)=5/5/1. (b) PLQY values of 2D CCP-HFFTP-PDAN (blue), 2D CCP-HFFTP-BDAN (red), and the reported small-molecule emitter 4CzIPN (black) after UV irradiation. The initial PLQY values were normalized to one. (c) The calculated distance between C=C bonds in adjacent layers of 2D CCP-PDAN (top) and 2D CCP-HFFTP-BDAN (bottom). Reproduced with permission from 33. Copyright © 2020, American Chemical Society.

#### 4. Magnetic Properties

In addition to possessing unique optoelectronic properties, V-2D-COFs are also interesting materials for the exploration of magnetic properties. For instance, the first investigation on the magnetic properties of a pyrene-based V-2D-COF ( $\text{sp}^2\text{c-COF}$ ) was reported in 2017 by Jiang et al.<sup>15</sup>  $\text{sp}^2\text{c-COF}$  with a tetragonal topology was synthesized via Knoevenagel polycondensation between  $\text{D}_{2h}$ -symmetric 1,3,6,8-tetrakis(4-formylphenyl)pyrene (TFPPy, **9**) and  $\text{C}_2$ -symmetric PDAN (**2**) with NaOH as the base (Figure 8). The energy level of the highest occupied molecular orbital (HOMO) is -5.74 eV, which makes  $\text{sp}^2\text{c-COF}$  can be oxidized by  $\text{I}_2$ , forming radicals which are localized at the pyrene knots.<sup>42</sup> The two-probe measurement of the oxidized  $\text{sp}^2\text{c-COF}$  demonstrated a conductivity of  $7.1 \times 10^{-2} \text{ Sm}^{-1}$ , which is 12 orders of magnitude higher than that of pristine  $\text{sp}^2\text{c-COF}$  ( $6.1 \times 10^{-14} \text{ Sm}^{-1}$ ). Moreover, electron spin resonance (ESR) spectroscopy of the oxidized  $\text{sp}^2\text{c-COF}$  displayed a g-factor of 2.0023. The intensity of g-factor was 120 and 25 times higher than those of the linear cyano-substituted vinylene-linked polymer and imine-linked COF analog at room temperature. Moreover, the saturated ESR intensity of the oxidized  $\text{sp}^2\text{c-CMP}$  is only 20% of that of  $\text{sp}^2\text{c-COF}$  which indicates that the crystallinity is also crucial for the formation of a dense spin system.

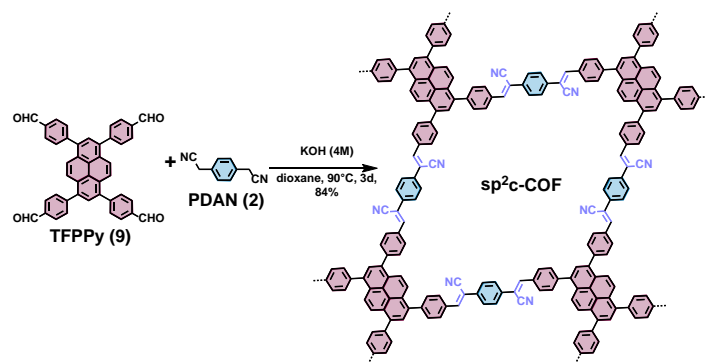


**Figure 8.** Synthesis of  $\text{sp}^2\text{c-COF}$  via Knoevenagel condensation of TFPPy (**9**) and PDAN (**2**).

## 5. Applications

### 5.1 Molecular Sensing

The combination of remarkable luminescent properties and a permanent porous structure make V-2D-COFs appealing materials for the molecular sensing of guest molecules, such as metal ions, where the pore can accommodate the guest molecules. The docking of these guest molecules subsequently triggers a change in the fluorescence of the V-2D-COFs for sensing.

Nuclear energy has played a critical role in the global energy system, but it poses potential environmental hazards because a large amount of radioactive uranium ( $\text{UO}_2^{2+}$ ) has been released into the environment. Thus,  $\text{UO}_2^{2+}$  detection and subsequent extraction from water are highly significant for environmental monitoring and protection. For the detection of  $\text{UO}_2^{2+}$ , the sensing materials must be highly robust against radioactivity and strong acids. In 2020, an amidoxime-substituted V-2D-COF (TFPT-BTAN-AO) was prepared by postmodification of cyano-substituted V-2D-COF (TFPT-BTAN) with  $\text{NH}_2\text{OH}\cdot\text{HCl}$  (Figure 9a).<sup>17</sup> The TFPT-BTAN-AO exhibited excellent chemical, thermal and radiation stability even by the treatment with water (100 °C), HCl (1 M),  $\text{HNO}_3$  (0.1~5.0 M), NaOH (1 M), and  $\gamma$ -ray radiation (50 kGy, 200 kGy). Moreover, TFPT-BTAN-AO showed an exceptional  $\text{UO}_2^{2+}$  adsorption capacity of 427  $\text{mg g}^{-1}$ , which can be attributed to the abundant selective uranium-binding amidoxime substituents on the highly accessible pore walls of open 1D channels (Figure 9b). In addition to the extraction of  $\text{UO}_2^{2+}$ , TFPT-BTAN-AO also allowed monitoring of the quality of the extracted water in view of the ultrafast response time (2 s) and an ultralow detection limit of 6.7 nM  $\text{UO}_2^{2+}$  (Figure 9c).

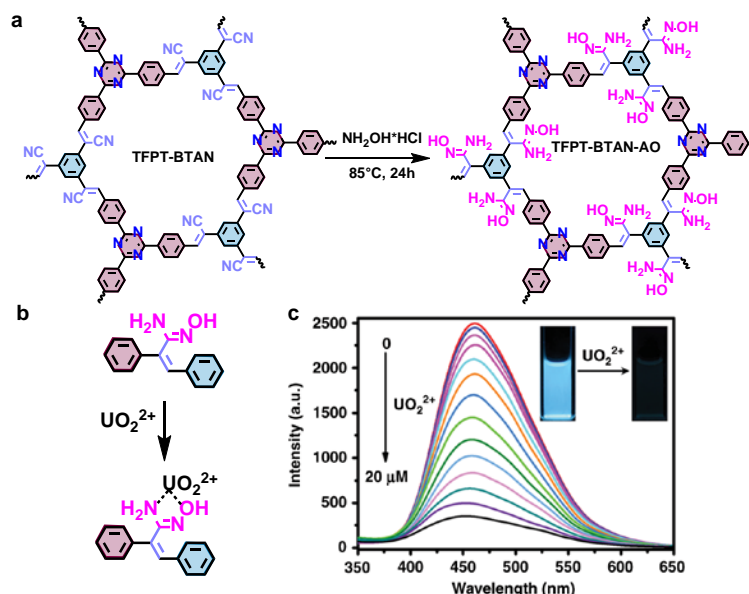


**Figure 9.** (a) The synthesis of amidoxime-substituted TFPT-BTAN-AO via postmodification of TFPT-BTAN. (b) The intermolecular interaction between amidoxime groups and  $\text{UO}_2^{2+}$ . (c) Fluorescence spectra and photographs of TFPT-BTAN-AO upon gradual addition of  $\text{UO}_2^{2+}$ .

## 5.2. Energy Storage

The incorporation of redox-active monomers into robust V-2D-COFs is highly desirable for the development of novel electrode materials for energy storage applications due to the following advantages: (1) the layered and porous structure of V-2D-COFs can deliver both ions and electrons along the stacking directions and within the layers; (2) the shape-persistent framework of V-2D-COFs has high (electro)chemical stability, which is crucial for long-term operation at accelerated current densities. In 2019, we incorporated an electrochemically active HATN monomer (HATN-6CHO, 10) for the synthesis of nitrogen-rich V-2D-COFs.<sup>9</sup> The prepared 2D CCP-HATN exhibited high chemical and electrochemical stability compared with its corresponding imine-linked analog (2D C=N HATN) (Figure 10a). By further enhancing the conductivity via in situ growth of 2D CCP-HATN on carbon nanotubes (CNTs), the resultant 2D CCP-HATN@CNT

core-shell hybrids demonstrated a high capacity of 116 mA h/g, superb cycling stability (91% capacity retention after 1000 cycles), and excellent rate capability (82%, 1.0 A/g vs 0.1 A/g) as a cathode material for lithium-ion batteries (LIBs) (Figure 10c and 10d).

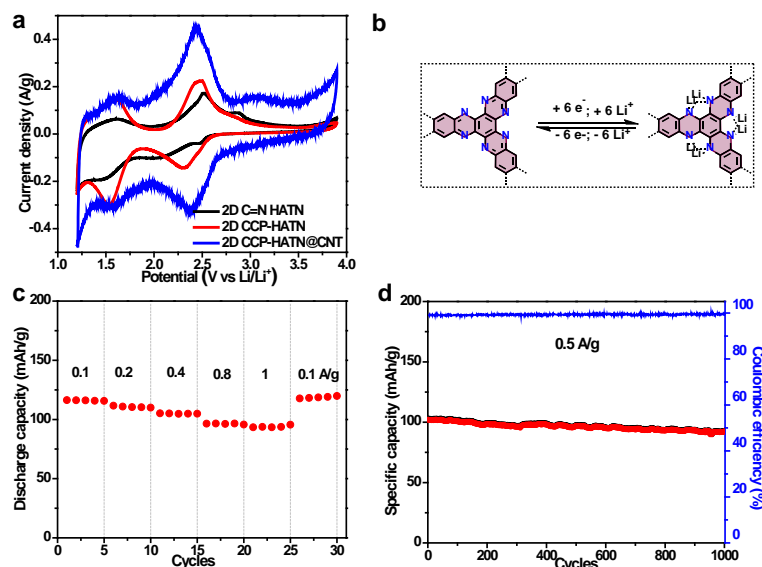


**Figure 10.** (a) Cyclic voltammetry of 2D C=N-HATN, 2D CCP-HATN and 2D CCP-HATN@CNT. (b) Proposed Li-ion storage of the redox-active HATN motif. (c) Charge-discharge profile of 2D CCP-HATN@CNT. (d) Cycling performance of 2D CCP-HATN@CNT at 0.5 A g<sup>-1</sup>; Reproduced with permission from 9. Copyright © 2019 Wiley-VCH Verlag GmbH & Co. KGaA, Weinheim.

In addition to its application in LIBs, V-2D-COF has also been demonstrated as an electrode material for micro supercapacitors (MSCs) with a high-rate capability and long-term cycling stability. For instance, a hybrid material composed of single-walled carbon nanotubes and unsubstituted V-2D-COF, namely, g-C<sub>34</sub>N<sub>6</sub>-COF, was integrated into a COF-based MSC.<sup>29</sup> The fabricated MSC device exhibited excellent areal capacitances of up to 15.2 mF cm<sup>-2</sup>, high energy

densities of up to  $7.3 \text{ mWh cm}^{-3}$ , and a remarkable rate capability with a capacitance retention of 45% when the current density was increased from  $0.05$  to  $5 \text{ mA cm}^{-2}$ .<sup>29</sup>

### 5.3 Photocatalysis

V-2D-COFs with high in-plane  $\pi$ -conjugation along both the x and y directions, narrow energy gaps, broad UV-vis absorption, high chemical stability and porous layered structures are auspicious materials for photocatalytic reactions. To date, a few V-2D-COFs have already been demonstrated as photocatalysts for different organic reactions.

In 2019, a porphyrin-incorporated V-2D-COF, namely, Por-sp<sup>2</sup>c-COF, was synthesized (Figure 11a) and used as a metal-free photocatalyst for visible-light-induced aerobic oxidation of amines into imines (Figure 11b).<sup>25</sup> By using Por-sp<sup>2</sup>c-COF as a photocatalyst, the oxidation reaction could be promoted with imine yields of up to 99%. Further ESR experiments indicated that the photocatalytic reactions involved key light-activated generation and separation of electron-hole pairs. In detail, an electron reacted with oxygen and formed a superoxide, while the hole oxidized on the amine substrates. In contrast, the corresponding imine-based Por-COF exhibited a lower conversion yield of ~44% for the imines. Therefore, the fully  $\pi$ -conjugated skeleton of V-2D-COFs enabled enhanced photocatalytic efficiency by facilitating the electron-transfer process.

Moreover, V-2D-COFs were also reported as photocatalysts for the aerobic photocatalytic transformation of arylboronic acids to phenols (Figure 11c and 11d).<sup>22</sup> Three unsubstituted V-2D-COFs (COF-*p*-3Ph, COF-*p*-2Ph, and COF-*m*-3Ph) were synthesized by aldol-type polycondensation between TCM (30) and PAD (28), BPDA (14) and DFPTP (27), respectively. As an example, the synthesis of COF-*m*-3Ph is displayed in Figure 11c. COF-*p*-3Ph, COF-*p*-2Ph, and COF-*m*-3Ph showed conduction band minimum (ECB) values of -3.8, -4.1, and -3.7 eV,

respectively. The ECB values are higher than the potential of  $O_2/O_2^-$  (4.16 eV), which enables the reduction of oxygen to a superoxide radical anion under appropriate photoirradiation conditions. As a result, all three V-2D-COFs could function as photocatalysts for the transformation of arylboronic acids into phenols. In particular, COF-*p*-3Ph provided photocatalytic yields of up to 99% (Figure 11d). The catalyst could be readily recycled via filtration and reused, demonstrating negligible decay of either photocatalytic activity or crystallinity after 10 recycling cycles.

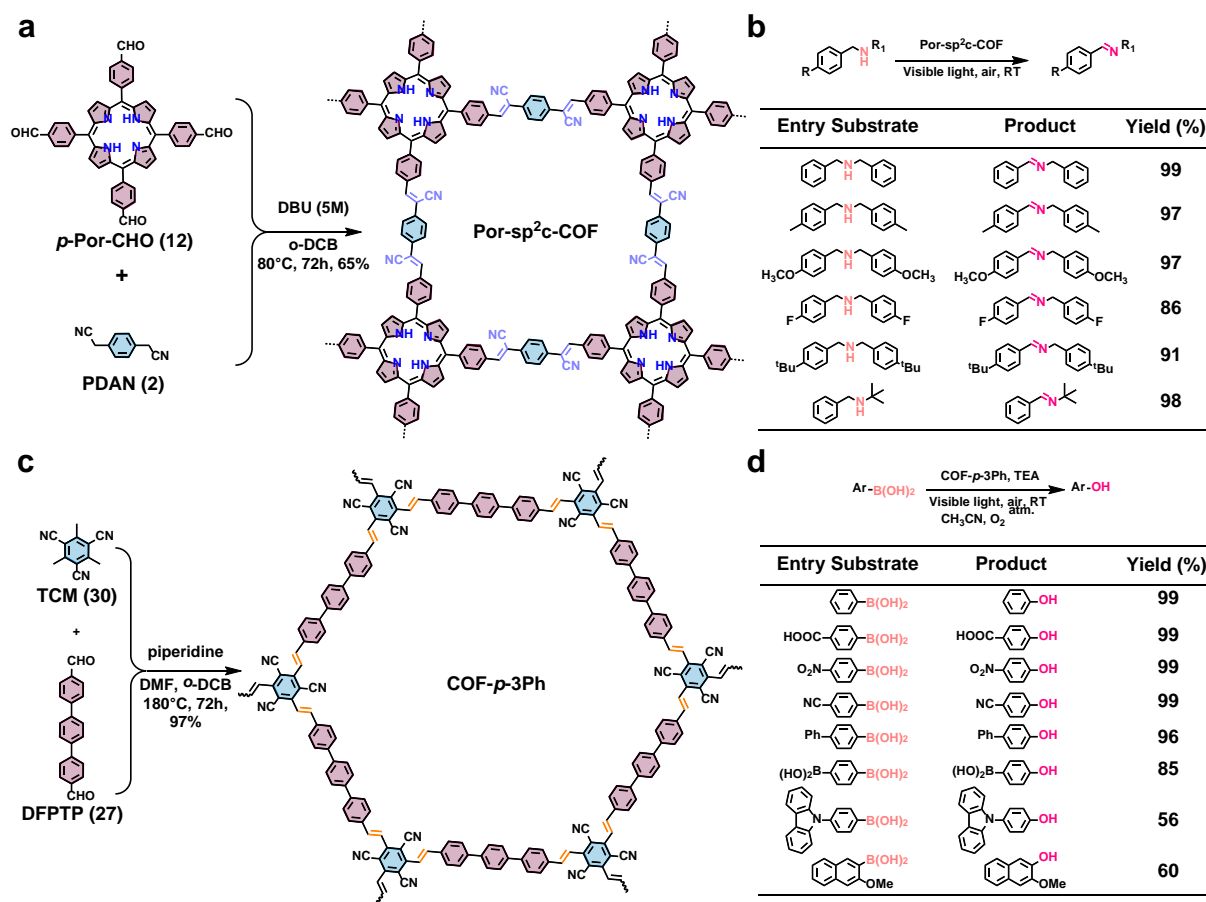


**Figure 11.** (a) Synthesis of Por-sp<sup>2</sup>c-COF from p-Por-CHO (12) and PDAN (2). (b) Por-sp<sup>2</sup>c-COF can serve as a metal-free photocatalyst for visible-light-induced aerobic oxidation of amines to imines. (c) Synthesis of COF-*p*-3Ph via Knoevenagel polycondensation between TCM (30) and

DFPTP (27). (d) The synthesized COF-*p*-3Ph is a photocatalyst for the aerobic photocatalytic transformation of aryl-boronic acids to phenols.

Natural photosynthesis with photosystem I can store the solar energy via the reduction of the coenzyme nicotinamide adenine dinucleotide phosphate (NADP) into NAD(P)H. The resulting NAD(P)H can be further consumed in several biochemical transformations, such as the production of carbohydrates via the Calvin cycle or the synthesis of L-glutamate from  $\alpha$ -ketoglutarate via dehydrogenase. In 2019, a cyano-substituted and triazine-contained 2D V-COF (TP-COF) was reported by the Knoevenagel polymerization between TFPT (11) and PDAN (2) (Figure 12a).<sup>26</sup> The incorporation of electron-withdrawing triazine units into TP-COF led to a tailoring of the optoelectronic properties with an optical band gap of 2.36 eV and a lowest unoccupied molecular orbital (LUMO) energy level of -3.23 eV. Under light irradiation, TP-COF collected the solar energy in form of excited electrons. Employing the electron mediator [Cp\*Rh(bpy)(H)]<sup>+</sup> (Represented as M in Figure 12b), electrons could be converted into NADH. Subsequently, together with L-glutamate dehydrogenase (GDH), the generated NADH catalyzed the conversion of  $\alpha$ -ketoglutarate into L-glutamate with an unprecedented high yield of 97% in 12 min.<sup>26</sup>

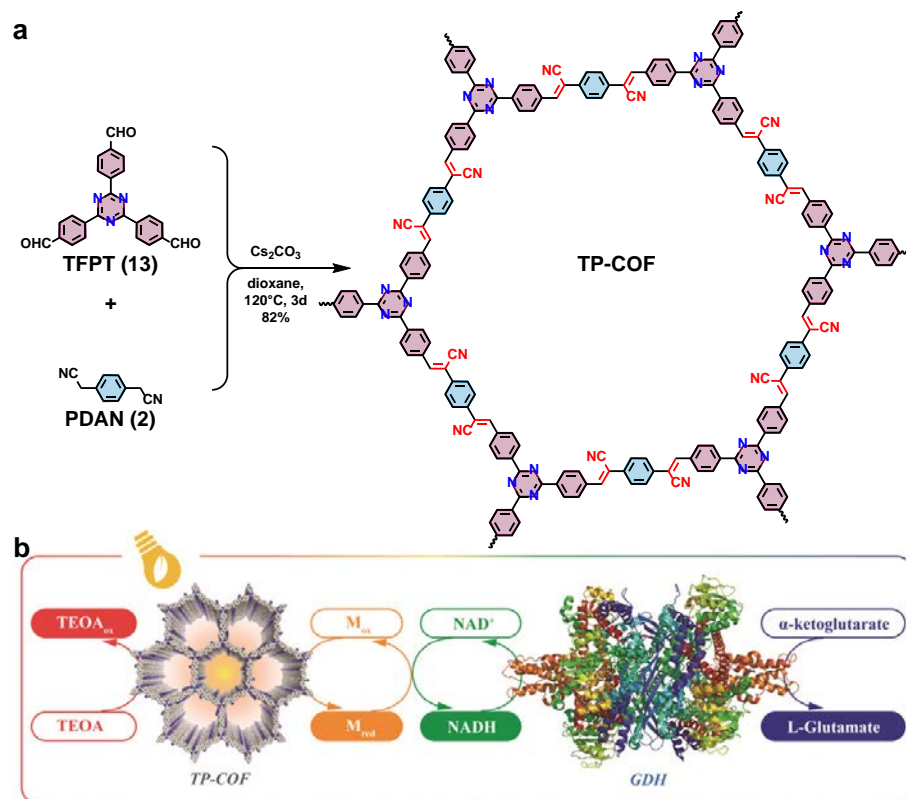


**Figure 12.** (a) Synthesis of TP-COF via Knoevenagel condensation between TFPT (11) and PDAN (2). (b) Illustration of the artificial PSI-induced coenzyme regeneration and photoenzymatic synthesis of L-glutamate by L-glutamate dehydrogenase (GDH). Reproduced with permission from reference 26. Copyright © 2019 Wiley-VCH Verlag GmbH & Co. KGaA, Weinheim.

#### 5.4. Photoelectrochemical (PEC) Water Reduction

Photoelectrochemical (PEC) water reduction allows the conversion of solar energy into hydrogen fuel by the use of a PEC water splitting cell. To achieve an attractive PEC performance, the semiconductor is required to have broad UV-vis absorption, efficient charge transfer, high

chemical and photostability, and a high lowest unoccupied molecular orbital (LUMO) energy level. The combination of aligned porous channels and tailored optoelectronic properties, such as the band gap or the energy level of frontier orbitals, makes V-2D-COFs promising materials for PEC water reduction.

The incorporation of donor and acceptor building blocks into conjugated polymers can lead to efficient charge transport and separation.<sup>43</sup> Recently, we developed a thiophene-bridged donor-acceptor-based V-2D-COF (2D CCP-HATN-ThDAN) via Knoevenagel polycondensation between the electron-deficient building block HATN-6CHO (10) and electron-donating thiophene-containing linker ThDAN (17) (Figure 13a).<sup>12</sup> In comparison to the biphenylene-bridged V-2D-COF (2D CCP-HATN-BDAN) analog and imine-linked 2D-c-COF (2D C=N HATN-BZD), the bithiophene-bridged 2D CCP-HATN-ThDAN showed a narrower optical energy bandgap of ~2.04 eV (Figure 13b), a higher LUMO energy level of -3.41 eV, and higher charge separation and transport. When applied as a photocathode for PEC water reduction, 2D CCP-HATN-ThDAN demonstrated a high saturated photocurrent density of up to 5.5  $\mu\text{A cm}^{-2}$  at 0.3 V and 7.9  $\mu\text{A cm}^{-2}$  at 0 V vs. the reversible hydrogen electrode (RHE) (Figure 13c), which is much higher than the performance of 2D C=N HATN-BZD (0.06  $\mu\text{A cm}^{-2}$ ) and 2D CCP-HATN-BDAN (2.8  $\mu\text{A cm}^{-2}$ ). DFT calculations further revealed that the sulfur atoms in the thiophene rings and the cyano groups at the vinylene linkage are the active sites for water reduction.

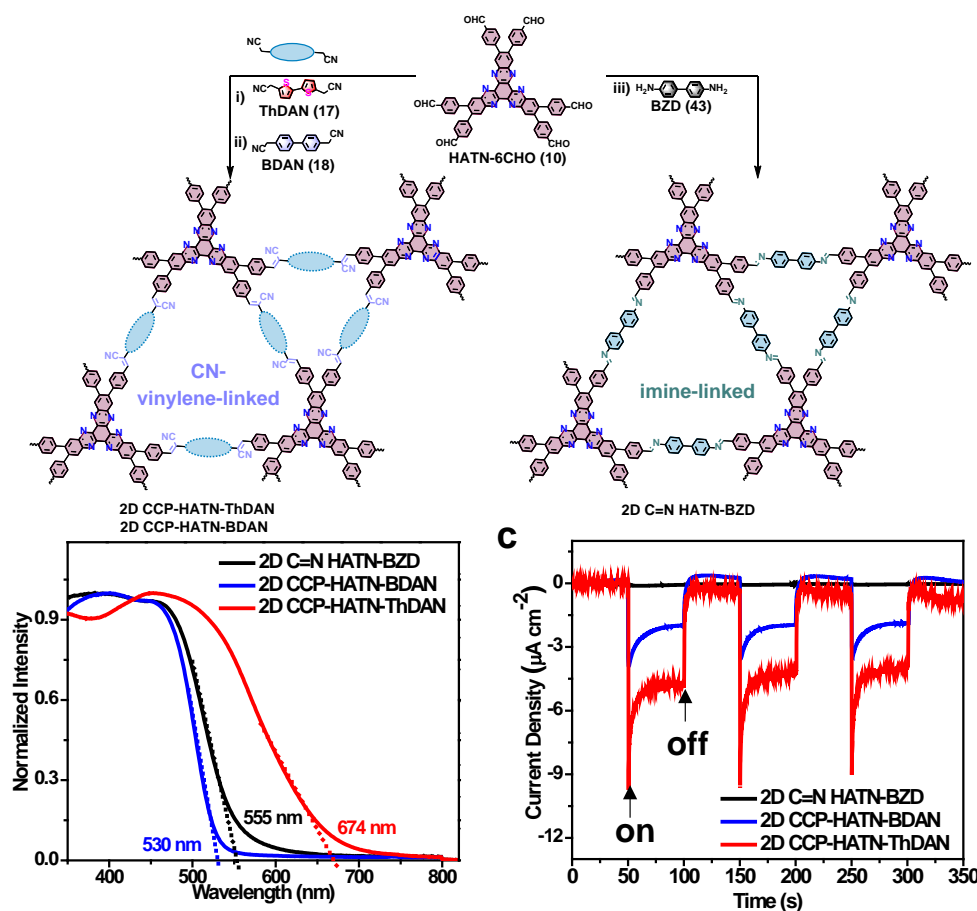


**Figure 13.** (a) Synthesis of 2D C=N HATN-BZD, 2D CCP-HATN-BDAN, and 2D CCP-HATN-ThDAN from HATN-6CHO (10). (b) UV-vis absorption spectrum (c) Photocurrent-time plots of 2D CCP-HATN-ThDAN (red line), 2D CCP-HATN-BDAN (blue line) and 2D C=N HATN-BZD (black line). On: illumination on; off: illumination off. Reproduced with permission from 12. Copyright © 2020 Wiley-VCH GmbH.

## 6. Summary

In the last five years, V-2D-COFs have been established as a remarkable class of COF materials due to their extended in-plane  $\pi$ -conjugation associated with unique physicochemical properties. In this Account, we have provided an overview of the recent developments in reaction

methodologies, design principles, optoelectronic and magnetic properties and functional applications for V-2D-COFs. Despite the rapid progress in this field, many issues remain to be addressed.

The major challenge remaining concerns the controlled synthesis of highly crystalline V-2D-COFs. Until now, compared to that of the corresponding imine-linked 2D-c-COF analogs, the crystallinity of V-2D-COFs has been generally low due to the intrinsic poor reversibility of C=C bond formation. Current studies of the mechanisms have demonstrated that the generation and stabilization of carbanion species, the choice of reaction conditions, and the design of suitable topological monomers are essential factors in the preparation of crystalline V-2D-COFs. However, a deep understanding and manipulation of the chemistry and the crystal-growth process are still missing, which will be essential for the future development of highly crystalline and even single-crystalline V-2D-COFs.

The formation of vinylene linkages in V-2D-COFs provides a remarkable  $\pi$ -conjugated scaffold, in contrast to imine-linked 2D-c-COFs. The excellent  $\pi$ -conjugation of V-2D-COFs is responsible for the resultant optoelectronic properties, such as high PLQY values. Further increasing the conjugation length/degree within the V-2D-COFs through the rational selection of suitable monomers or achieving maximized crystallinity (or polymerization degree) will be essential to make full use of their intrinsic physicochemical properties and to eventually bridge the world of 2D conjugated polymers with exceptional 2D conjugated pathways. Benefitting from designable and tailorable building blocks, topologies, porous properties, and redox properties, V-2D-COFs have already been demonstrated to be attractive materials for molecular sensing, photocatalysis, photoelectrochemical catalysis, energy storage, etc. Expanding the application scope of V-2D-COFs is expected to occur by the further development of robust synthetic methods and material

classes for this type of framework material. We expect that unprecedented V-2D-COF structures with unique properties will provide new opportunities to address some fundamental and global challenging questions ranging from optoelectronics to energy storage and conversion as well as biological applications.

## AUTHOR INFORMATION

### Corresponding Author

Xinliang Feng\*. Chair of Molecular Functional Materials, Technische Universität Dresden, Center for Advancing Electronics Dresden (cfaed) and Faculty of Chemistry and Food Chemistry, Mommsenstraße 4, 01069 Dresden (Germany). E-mail: [xinliang.feng@tu-dresden.de](mailto:xinliang.feng@tu-dresden.de)

### Author Contributions

The manuscript was written through contributions of all authors. All authors have given approval to the final version of the manuscript.

### Biographical sketches

**Shunqi Xu** received Bachelor degree in July 2013 from Southeast University. In July 2016, he got Master degree under the supervision of Professor Xin Zhao from Shanghai Institute of Organic Chemistry, University of Chinese Academy of Sciences. In September 2016, he joined the group of Prof. Xinliang Feng as a PhD student at the Chair of Molecular Functional Materials of Technische Universität Dresden (TUD). Currently, he is a postdoc in the Chair of Prof. Xinliang Feng working on the organic synthesis of novel 2D conjugated polymers as well as their applications in energy storage, photo(electrochemical)catalyst reactions, and optoelectronics.

**Marcus Richter** started his Chemistry studies at TU Dresden in 2009. Afterwards, he joined the group of Prof. Dr. Xinliang Feng as PhD student. During his PhD student time, his focus was the synthesis of polycyclic aromatic hydrocarbons (PAHs). Since 2019, he is the group leader of the 2D conjugated polymer subgroup at the Chair of Molecular Functional Materials at the TUD. His current research focus is the synthesis, characterization and application of novel 2D conjugated polymers and 2D COFs.

**Xinliang Feng** has been full professor and the head of the Chair of Molecular Functional Materials at Technische Universität Dresden since 2014. His current scientific interests include new polymer synthetic methodology, organic synthesis and supramolecular chemistry of  $\pi$ -conjugated systems, bottom-up synthesis of graphene and graphene nanoribbons, electrochemical exfoliation of 2D crystals, 2D polymers and 2D supramolecular polymers, as well as 2D carbon-rich conjugated polymers for opto-electronics, energy storage and conversion, and new energy devices and technologies.

## ACKNOWLEDGMENT

This work was supported financially by the EU Graphene Flagship (Graphene Core, No. 881603), the Collaborative Research Center (CRC) 1415 "Chemistry of Synthetic Two-Dimensional Materials" (No. 417590517), H2020-MSCA-ITN (ULTIMATE, No. 813036), the Center for Advancing Electronics Dresden (cfaed), and the ERC Consolidator Grant (T2DCP, No. 819698). We thank Dr. Naisa Chandrasekhar, Prof. Bishnu P. Biswal, M. Sc. Dominik Pasoetter and M. Sc. Albrecht Waentig for the helpful discussion.

## REFERENCES

- (1) Yu, M.; Dong, R.; Feng, X. Two-Dimensional Carbon-Rich Conjugated Frameworks for Electrochemical Energy Applications. *J. Am. Chem. Soc.* **2020**, *142*, 12903–12915.

- (2) Liang, R. R.; Jiang, S. Y.; A R.-H.; Zhao, X. Two-Dimensional Covalent Organic Frameworks with Hierarchical Porosity. *Chem. Soc. Rev.* **2020**, *49*, 3920–3951.
- (3) Chen, X.; Geng, K.; Liu, R.; Tan, K. T.; Gong, Y.; Li, Z.; Tao, S.; Jiang, Q.; Jiang, D. Covalent Organic Frameworks: Chemical Approaches to Designer Structures and Built-In Functions. *Angew. Chem. Int. Ed.* **2020**, *59*, 5050–5091.
- (4) Wan, S.; Gándara, F.; Asano, A.; Furukawa, H.; Saeki, A.; Dey, S. K.; Liao, L.; Ambrogio, M. W.; Botros, Y. Y.; Duan, X.; Seki, S.; Stoddart, J. F.; Yaghi, O. M. Covalent Organic Frameworks with High Charge Carrier Mobility. *Chem. Mater.* **2011**, *23*, 4094–4097.
- (5) Tian, Y.; Xu, S.-Q.; Liang, R.-R.; Qian, C.; Jiang, G.-F.; Zhao, X. Construction of Two Heteropore Covalent Organic Frameworks with Kagome Lattices. *CrystEngComm.* **2017**, *19*, 4877–4881.
- (6) Uribe-Romo, F. J.; Doonan, C. J.; Furukawa, H.; Oisaki, K.; Yaghi, O. M. Crystalline Covalent Organic Frameworks with Hydrazone Linkages. *J. Am. Chem. Soc.* **2011**, *133*, 11478–11481.
- (7) Dalapati, S.; Jin, S.; Gao, J.; Xu, Y.; Nagai, A.; Jiang, D. An Azine-Linked Covalent Organic Framework. *J. Am. Chem. Soc.* **2013**, *135*, 17310–17313.
- (8) Liang, R. R.; A, R.-H.; Xu, S.-Q.; Qi, Q.-Y.; Zhao, X. Fabricating Organic Nanotubes through Selective Disassembly of Two-Dimensional Covalent Organic Frameworks. *J. Am. Chem. Soc.* **2020**, *142*, 70–74.
- (9) Xu, S.; Wang, G.; Biswal, B. P.; Addicoat, M.; Paasch, S.; Sheng, W.; Zhuang, X.; Brunner, E.; Heine, T.; Berger, R.; Feng, X. A Nitrogen-Rich 2D Sp<sup>2</sup>-Carbon-Linked Conjugated Polymer Framework as a High-Performance Cathode for Lithium-Ion Batteries. *Angew. Chem. Int. Ed.* **2019**, *58*, 849–853.
- (10) Jin, E.; Geng, K.; Lee, K. H.; Jiang, W.; Li, J.; Jiang, Q.; Irle, S.; Jiang, D. Topology-Templated Synthesis of Crystalline Porous Covalent Organic Frameworks. *Angew. Chem. Int. Ed.* **2020**, *59*, 12162–12169.
- (11) Rao, M. R.; Fang, Y.; De Feyter, S.; Perepichka, D. F. Conjugated Covalent Organic Frameworks via Michael Addition-Elimination. *J. Am. Chem. Soc.* **2017**, *139*, 2421–2427.
- (12) Xu, S.; Sun, H.; Addicoat, M.; Biswal, B. P.; He, F.; Park, S. W.; Paasch, S.; Zhang, T.; Sheng, W.; Brunner, E.; Hou, Y.; Richter, M.; Feng, X. Thiophene-Bridged Donor–Acceptor Sp<sup>2</sup>-Carbon-Linked 2D Conjugated Polymers as Photocathodes for Water Reduction. *Adv. Mater.* **2021**, *33*, 2006274.
- (13) Sahabudeen, H.; Qi, H.; Ballabio, M.; Položij, M.; Olthof, S.; Shivhare, R.; Jing, Y.; Park, S. W.; Liu, K.; Zhang, T.; Ma, J.; Rellinghaus, B.; Mannsfeld, S.; Heine, T.; Bonn, M.; Cunovas, E.; Zheng, Z.; Kaiser, U.; Dong, R.; Feng, X. Highly Crystalline and Semiconducting Imine-Based Two-Dimensional Polymers Enabled by Interfacial Synthesis. *Angew. Chem. Int. Ed.* **2020**, *59*, 6028–6036.

- (14) Zhuang, X.; Zhao, W.; Zhang, F.; Cao, Y.; Liu, F.; Bi, S.; Feng, X. A Two-Dimensional Conjugated Polymer Framework with Fully Sp<sup>2</sup>-Bonded Carbon Skeleton. *Polym. Chem.* **2016**, *7*, 4176–4181.
- (15) Jin, E.; Asada, M.; Xu, Q.; Dalapati, S.; Addicoat, M. A.; Brady, M. A.; Xu, H.; Nakamura, T.; Heine, T.; Chen, Q.; Jiang, D. Two-Dimensional Sp<sup>2</sup> Carbon-Conjugated Covalent Organic Frameworks. *Science*. **2017**, *357*, 673–676.
- (16) Jin, E.; Li, J.; Geng, K.; Jiang, Q.; Xu, H.; Xu, Q.; Jiang, D. Designed Synthesis of Stable Light-Emitting Two-Dimensional Sp<sup>2</sup> Carbon-Conjugated Covalent Organic Frameworks. *Nat. Commun.* **2018**, *9*, 4143.
- (17) Cui, W. R.; Zhang, C. R.; Jiang, W.; Li, F. F.; Liang, R. P.; Liu, J.; Qiu, J.-D. Regenerable and Stable Sp<sup>2</sup> Carbon-Conjugated Covalent Organic Frameworks for Selective Detection and Extraction of Uranium. *Nat. Commun.* **2020**, *11*, 436.
- (18) Jin, E.; Lan, Z.; Jiang, Q.; Geng, K.; Li, G.; Wang, X.; Jiang, D. 2D Sp<sup>2</sup> Carbon-Conjugated Covalent Organic Frameworks for Photocatalytic Hydrogen Production from Water. *Chem* **2019**, *5*, 1632–1647.
- (19) Liang, R. R.; Xu, S.-Q.; Zhang, L.; A, R.-H.; Chen, P.; Cui, F.-Z.; Qi, Q.-Y.; Sun, J.; Zhao, X. Rational Design of Crystalline Two-Dimensional Frameworks with Highly Complicated Topological Structures. *Nat. Commun.* **2019**, *10*, 4609.
- (20) Lyu, H.; Diercks, C. S.; Zhu, C.; Yaghi, O. M. Porous Crystalline Olefin-Linked Covalent Organic Frameworks. *J. Am. Chem. Soc.* **2019**, *141*, 6848–6852.
- (21) Bi, S.; Yang, C.; Zhang, W.; Xu, J.; Liu, L.; Wu, D.; Wang, X.; Han, Y.; Liang, Q.; Zhang, F. Two-Dimensional Semiconducting Covalent Organic Frameworks via Condensation at Arylmethyl Carbon Atoms. *Nat. Commun.* **2019**, *10*, 2467.
- (22) Bi, S.; Thiruvengadam, P.; Wei, S.; Zhang, W.; Zhang, F.; Gao, L.; Xu, J.; Wu, D.; Chen, J.-S.; Zhang, F. Vinylene-Bridged Two-Dimensional Covalent Organic Frameworks via Knoevenagel Condensation of Tricyanomesitylene. *J. Am. Chem. Soc.* **2020**, *142*, 11893–11900.
- (23) Pastoetter, D. L.; Xu, S.; Borrelli, M.; Addicoat, M.; Biswal, B. P.; Paasch, S.; Dianat, A.; Thomas, H.; Berger, R.; Reineke, S.; Brunner, E.; Cuniberti, G.; Richter, M.; Feng, X. Synthesis of Vinylene-Linked Two-Dimensional Conjugated Polymers via the Horner–Wadsworth–Emmons Reaction. *Angew. Chem. Int. Ed.* **2020**, *59*, 23620–23625.
- (24) Becker, D.; Biswal, B. P.; Kaleńczuk, P.; Chandrasekhar, N.; Giebeler, L.; Addicoat, M.; Paasch, S.; Brunner, E.; Leo, K.; Dianat, A.; Cuniberti, G.; Berger, R.; Feng, X. Fully Sp<sup>2</sup> -Carbon-Linked Crystalline Two-Dimensional Conjugated Polymers: Insight into 2D Poly(Phenylenecyanovinylene) Formation and Its Optoelectronic Properties. *Chem. Eur. J.* **2019**, *25*, 6562–6568.

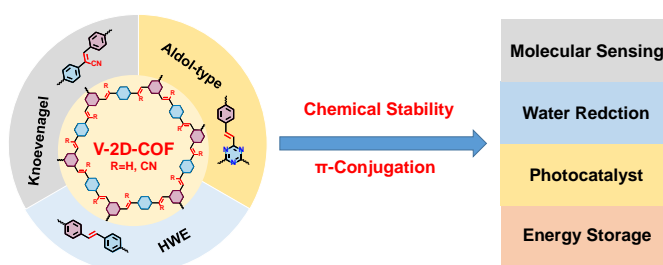
- (25) Chen, R.; Shi, J.-L.; Ma, Y.; Lin, G.; Lang, X.; Wang, C. Designed Synthesis of a 2D Porphyrin-Based  $Sp^2$  Carbon-Conjugated Covalent Organic Framework for Heterogeneous Photocatalysis. *Angew. Chem. Int. Ed.* **2019**, *58*, 6430–6434.
- (26) Zhao, Y.; Liu, H.; Wu, C.; Zhang, Z.; Pan, Q.; Hu, F.; Wang, R.; Li, P.; Huang, X.; Li, Z. Fully Conjugated Two-Dimensional  $Sp^2$ -Carbon Covalent Organic Frameworks as Artificial Photosystem I with High Efficiency. *Angew. Chem. Int. Ed.* **2019**, *58*, 5376–5381.
- (27) Fu, Z.; Wang, X.; Gardner, A. M.; Wang, X.; Chong, S. Y.; Neri, G.; Cowan, A. J.; Liu, L.; Li, X.; Vogel, A.; Clowes, R.; Bilton, M.; Chen, L.; Sprick, R. S.; Cooper, A. I. A Stable Covalent Organic Framework for Photocatalytic Carbon Dioxide Reduction. *Chem. Sci.* **2020**, *11*, 543–550.
- (28) Acharjya, A.; Longworth-Dunbar, L.; Roeser, J.; Pachfule, P.; Thomas, A. Synthesis of Vinylene-Linked Covalent Organic Frameworks from Acetonitrile: Combining Cyclotrimerization and Aldol Condensation in One Pot. *J. Am. Chem. Soc.* **2020**, *142*, 14033–14038.
- (29) Xu, J.; He, Y.; Bi, S.; Wang, M.; Yang, P.; Wu, D.; Wang, J.; Zhang, F. An Olefin-Linked Covalent Organic Framework as a Flexible Thin-Film Electrode for a High-Performance Micro-Supercapacitor. *Angew. Chem. Int. Ed.* **2019**, *58*, 12065–12069.
- (30) Wei, S.; Zhang, F.; Zhang, W.; Qiang, P.; Yu, K.; Fu, X.; Wu, D.; Bi, S.; Zhang, F. Semiconducting 2D Triazine-Cored Covalent Organic Frameworks with Unsubstituted Olefin Linkages. *J. Am. Chem. Soc.* **2019**, *141*, 14272–14279.
- (31) Acharjya, A.; Pachfule, P.; Roeser, J.; Schmitt, F.-J.; Thomas, A. Vinylene-Linked Covalent Organic Frameworks by Base-Catalyzed Aldol Condensation. *Angew. Chem. Int. Ed.* **2019**, *58*, 14865–14870.
- (32) Jadhav, T.; Fang, Y.; Patterson, W.; Liu, C.-H.; Hamzehpoor, E.; Perepichka, D. F. 2D Poly(Arylene Vinylene) Covalent Organic Frameworks via Aldol Condensation of Trimethyltriazine. *Angew. Chem. Int. Ed.* **2019**, *58*, 13753–13757.
- (33) Xu, S.; Li, Y.; Biswal, B. P.; Addicoat, M. A.; Paasch, S.; Imbrasas, P.; Park, S.; Shi, H.; Brunner, E.; Richter, M.; Lenk, S.; Reineke, S.; Feng, X. Luminescent  $Sp^2$ -Carbon-Linked 2D Conjugated Polymers with High Photostability. *Chem. Mater.* **2020**, *32*, 7985–7991.
- (34) Li, X.; Gao, Q.; Wang, J.; Chen, Y.; Chen, Z.-H.; Xu, H.-S.; Tang, W.; Leng, K.; Ning, G.-H.; Wu, J.; Xu, Q.-H.; Quek, S. Y.; Lu, Y.; Loh, K. P. Tuneable near White-Emissive Two-Dimensional Covalent Organic Frameworks. *Nat. Commun.* **2018**, *9*, 2335.
- (35) Ding, S.-Y.; Dong, M.; Wang, Y.-W.; Chen, Y.-T.; Wang, H.-Z.; Su, C.-Y.; Wang, W. Thioether-Based Fluorescent Covalent Organic Framework for Selective Detection and Facile Removal of Mercury(II). *J. Am. Chem. Soc.* **2016**, *138*, 3031–3037.
- (36) Haldar, S.; Chakraborty, D.; Roy, B.; Banappanavar, G.; Rinku, K.; Mullangi, D.; Hazra, P.; Kabra, D.; Vaidhyanathan, R. Anthracene-Resorcinol Derived Covalent Organic Framework as Flexible White Light Emitter. *J. Am. Chem. Soc.* **2018**, *140*, 13367–13374.

- (37) Albacete, P.; Martínez, J. I.; Li, X.; López-Moreno, A.; Mena-Hernando, S.; Platero-Prats, A. E.; Montoro, C.; Loh, K. P.; Pérez, E. M.; Zamora, F. Layer-Stacking-Driven Fluorescence in a Two-Dimensional Imine-Linked Covalent Organic Framework. *J. Am. Chem. Soc.* **2018**, *140*, 12922–12929.
- (38) Li, Z.; Huang, N.; Lee, K. H.; Feng, Y.; Tao, S.; Jiang, Q.; Nagao, Y.; Irle, S.; Jiang, D. Light-Emitting Covalent Organic Frameworks: Fluorescence Improving via Pinpoint Surgery and Selective Switch-On Sensing of Anions. *J. Am. Chem. Soc.* **2018**, *140*, 12374–12377.
- (39) Li, Z.; Zhang, Y.; Xia, H.; Mu, Y.; Liu, X. A Robust and Luminescent Covalent Organic Framework as a Highly Sensitive and Selective Sensor for the Detection of Cu<sup>2+</sup> ions. *Chem. Commun.* **2016**, *52*, 6613–6616.
- (40) Shahid, I. Failure Analysis of Tools. *Adv. Mater. Process.* **2004**, *162*, 51.
- (41) Jadhav, T.; Fang, Y.; Liu, C.-H.; Dadvand, A.; Hamzehpoor, E.; Patterson, W.; Jonderian, A.; Stein, R. S.; Perepichka, D. F. Transformation between 2D and 3D Covalent Organic Frameworks via Reversible [2 + 2] Cycloaddition. *J. Am. Chem. Soc.* **2020**, *142*, 8862–8870.
- (42) Yu, H.; Wang, D. Metal-Free Magnetism in Chemically Doped Covalent Organic Frameworks. *J. Am. Chem. Soc.* **2020**, *142*, 11013–11021.
- (43) Pachfule, P.; Acharjya, A.; Roeser, J.; Sivasankaran, R. P.; Ye, M. Y.; Brückner, A.; Schmidt, J.; Thomas, A. Donor-Acceptor Covalent Organic Frameworks for Visible Light Induced Free Radical Polymerization. *Chem. Sci.* **2019**, *10*, 8316–8322.

## For Table of Contents Use Only:

# Vinylene-Linked Two-Dimensional Covalent Organic Frameworks: Synthesis and Functions

Shunqi Xu, Marcus Richter, Xinliang Feng \*



TOC